Casals M., Gangolells M., Forcada N., Macarulla M., Giretti A., Vaccarini M. SEAM4US: an intelligent energy management system for underground stations. *Applied Energy*, 2016, 166: 150-164. <doi:10.1016/j.apenergy.2016.01.029>

Final version available at: < http://www.sciencedirect.com/science/article/pii/S0306261916300095>.

# SEAM4US: an intelligent energy management system for underground stations

Miquel Casals [a], Marta Gangolells [a*], Núria Forcada [a], Marcel Macarulla [a], Alberto Giretti [b], Massimo Vaccarini [b]

[a] Universitat Politècnica de Catalunya, Department of Construction Engineering, Group of Construction Research and Innovation (GRIC), C/ Colom, 11, Ed. TR5, 08222 Terrassa (Barcelona), Spain

[b] Università Politecnica delle Marche, Department of Civil and Building Engineering and Architecture, Via delle Brecce Bianche, 60100 Ancona, Italy

[*] Corresponding author: Marta Gangolells. Tel: (+34) 93 7398947, Fax: (+34) 93 7398101. E-mail: marta.gangolells@upc.edu



## ABSTRACT

Several previous research initiatives have highlighted the role of Information and Communication Technologies (ICT) as key enablers for decreasing energy usage in buildings. However, few advances have been achieved in underground public spaces. This paper introduces a novel intelligent energy management system for underground stations. The system implements artificial intelligence solutions for autonomous building system control, based on advanced control algorithms that can learn from previous operations and situations. The robustness needed to operate in public spaces is achieved through a seamlessly integrated monitoring grid with self-diagnosis mechanisms. A middleware platform integrates existing devices, subsystems and newly deployed sensor-actuator networks. Results obtained during the implementation of the system in a prototype underground station showed potential yearly energy savings ranging between 74,336 and 87,339 kWh. The highest energy savings potential was found in the ventilation subsystem (30.6 % ± 2.0%), followed by the lighting system (24.1% ± 1.9%) and escalators (8.5% ± 1.9%).

*Keywords:*
energy management system, energy consumption, intelligent control, underground station, metro network

## 1. INTRODUCTION

Several previous research initiatives have highlighted the role of Information and Communication Technologies (ICT) as key enablers to decrease energy usage in buildings [1, 2, 3, 4, 5, 6, 7, 8] and thus, they can help us to attain the new targets set in the recently agreed 2030 climate and energy policy framework for the European Union [9]: a 27% improvement in energy efficiency, 27% of energy consumption from renewable resources, and a 40% reduction of greenhouse gas emissions by 2030, in

relation to 1990 levels. However and as shown by the in-depth reviews presented by Shaikh et al. [1], Beaudin et al. [2] and Khan et al. [3], most of the works performed focus on domestic energy management systems and leave undetermined how ICT systems can cope with different scales of buildings where the complexity of the optimisation increases [4]. Ongoing research efforts within the field of large scale public buildings mainly address hospitals, educational buildings, sport facilities, commercial buildings and offices. Papantoniou et al. [5] explicitly focused on an optimization and control algorithm integrated to the existing building management system of a hospital. Aghemo et al. [6] introduced intelligent energy consumption monitoring and control in educational buildings whereas Petri et al. [5] addressed sport facilities presenting a modular based optimisation system. Gulbinas et al. [7] developed a socio-technical building energy management system for commercial buildings and Garnier et al. [8] presented a predictive control strategy for existing zoned HVAC systems in non-residential buildings mainly devoted to administrative buildings. Key challenges of implementing intelligent energy management systems in large public spaces are mainly concerned with collecting real-time information related to occupancy, environmental conditions and energy consumption and integrated automation and control algorithms able to optimize control strategies in real-time. Insufficient interoperability preventing the collaboration among building subsystems, wireless sensor networks for large scale deployment and self-diagnosis to detect failures are also key aspects to be solved in such complex environments.

To the authors' knowledge, none of the previous initiatives has undertaken the energy optimization of underground stations, although they have been found to consume high levels of energy [10, 11] mostly due to their underground nature and the need to meet high safety, security, hygiene and comfort levels [12]. Besides being big energy consumers, control systems in public underground environments have tended to be based on legacy on/off schedules [13] and synergies with the external environmental climate and interaction with occupancy patterns and train arrivals have not been explored.

Within this context, the aim of this paper is to present a novel, advanced intelligent energy management system for underground stations. Autonomous building system control is achieved without diminishing current passenger comfort levels. According to the metro operator's requirements, the system allows the default control and corresponding conditions to be restored at any time. The system is integrated with existing subsystems in the underground station and implementation costs are as low as possible. In addition, the solution is robust enough to be implemented in underground public spaces. The system was deployed and evaluated in a prototype underground station that is part of the Barcelona metro network. After describing the method adopted within this research, Section 3 discusses the results obtained during the pilot implementation and gives evidence of the energy savings that were achieved. Finally, Section 4 describes the conclusions and future steps that could be taken.

## 2. RESEARCH METHOD

The research method used in this study included the following steps:

- Definition of control policies
- Development of environmental and occupancy models

- Integration of the system
- Pilot implementation

## 2.1. DEFINITION OF CONTROL POLICIES

Control policies were defined in accordance with the results obtained during the energy audit of the prototype underground station [14]. With an average consumption of 217.64 kWh/m$^2$·year, the breakdown revealed that the lighting system (37%), dominated the underground station's energy consumption, mainly because underground spaces cannot take advantage of natural lighting. A significant amount of energy (14%) was also found to be used for ventilation purposes. Ventilation systems are used to reduce the concentration of various pollutants in underground stations [15] and thus, to guarantee indoor air quality. Ventilation is also used to control internal temperature, which is affected by highly variable internal gains due to travelling passengers and trains (the piston effect), intricate air exchange dynamics with the outside, and heat conduction though the surrounding soil [16]. The vertical transportation system required for massive passenger flow in multi-storey spaces was found to account for 8% of the energy consumption of the underground station. The rest of the energy consumption was attributed to illuminated advertising signs (14%), mobile phone signal antenna (12%), small power devices (5%), air conditioning systems in staff and technical rooms (4%), vending machines (3%), ticketing and validation machines (1%) and LCD monitors (<1%) [14]. Systems that are not directly controlled by the metro operator, such as illuminated advertising signs or the mobile phone signal antenna, were excluded. Thus, the new control system acted on the lighting, ventilation and vertical transportation subsystems, which accounted for 72.54% of the energy consumed within the public spaces of the prototype underground station. Elevators were excluded, because they were found to use top-of-the range technology already. In all cases, the control policies were defined to ensure that passenger comfort does not diminish, and the actuations do not modify the current operator's controllers' tasks.

### 2.1.1 Lighting system

Current regulations [17, 18] establish minimum illuminance levels in underground stations, according to the difficulty of the visual task that must be performed in each area. In general, halls must have a minimum illuminance level of 200 lux, except in areas where tickets are sold and validation machines are situated, where the minimum illuminance level is 300 lux. A lower illuminance level is allowed in corridors (100 lux), although stairs and ramps must have a minimum illuminance level of 150 lux. Finally, and according to current regulations [17, 18], the required illuminance level on platforms must range between 150 lux (general) and 200 lux (platform edges).

The prototype underground station is illuminated by 400 fixtures hosting two 36W T8 fluorescents lamps with standard electronic ballasts. For safety reasons, a total of 110 emergency lights are also distributed around the station. Field illuminance testing in the pilot underground station indicated that current illuminance levels were significantly higher than the levels stated in the regulations. As an example, the average illuminance level of station halls was found to be between 32% and 68% higher than required by current regulations. Similar, even higher percentages were found in ticket sale and ticket

validation machine areas (30%-126%); corridors, including stairs and ramps (21%-220%); and platforms (19%-91%). This can be attributed not only to safety, security and aesthetics [15], but also to oversized dimensioning to overcome future aging and dirtiness. Moreover, existing fluorescent lights were changed for others that provide higher illuminance levels using the same fixtures. The lighting system was initially managed following a pre-defined schedule in which lights remain on when the station is open (150 hours per week).

For the purpose of this research, two main classes of visual tasks for passengers travelling through a metro station were distinguished: (1) visual tasks related to specific operations and (2) visual tasks concerned with movement. Visual tasks related to specific operations such as buying and validating tickets and operating train doors from the platform determine the minimum illuminance level requirements. Visual tasks concerned with movement require a clear perception of the floor, of trains and of other passengers. During non-rush hours, a clear recognition of other passengers' faces is important to enhance the sense of security when the platform is almost empty. During rush hours, the visual horizon of a travelling passenger is much shorter because of the crowd and thus, faces of surrounding passengers can be recognized easier. Therefore, visual tasks concerning movement require higher illuminance levels during non-rush hours whereas the same tasks can be carried out with less illuminance during rush hours.

In light of the abovementioned, the lighting level of public spaces during rush hours is set to the minimum stated by current regulations [17, 18]:

$$L = L_{min} \quad [1]$$

Where:

L is the lighting level expressed in lux, and $L_{min}$ is the minimum lighting level set by current regulations [17, 18] expressed in lux.

When the station is outside of rush hours, the lighting level is increased towards the maximum lighting level using the following equation:

$$L = L_{max} - \frac{(L_{max} - L_{min}) \cdot N}{N_{max}} \quad [2]$$

Where:

L is the lighting level expressed in lux, $L_{min}$ is the minimum lighting level set by current regulations [17, 18] expressed in lux, $L_{max}$ is the maximum lighting level expressed in lux and corresponds to the lighting level currently achieved within the station, N denotes the number of people in the controlled space, and $N_{max}$ is the maximum number of people in the controlled space during rush hours.

Rush hours are established by analysing the station's historical occupancy data, which is periodically updated with occupancy data retrieved from the closed-circuit television (CCTV) system. The occupancy threshold is defined as 65% of the maximum occupancy level expected for the day. Table 1 summarizes the adopted lighting control

policies. In order to make lighting variations unperceivable, the lighting level is filtered and smoothed prior to its application to the lighting system.

| Area | Illuminance levels during rush hours [lux] | Illuminance levels during non-rush hours[1] [lux] |
|---|---|---|
| Platform | Lighting level = 77%<br><br>Platform (edge) = 200 lux<br>Platform (center) = 150 lux<br>Platform (wall) = 200 lux | Lighting level = 100%<br><br>Platform (edge) = 327 lux<br>Platform (center) = 299 lux<br>Platform (wall) = 432 lux |
| Halls | Lighting level = 53%<br><br>Halls (ticket selling and validation machines) = 300 lux<br>Halls (general) = 200 lux | Lighting level = 100%<br><br>Halls (ticket selling and validation machines) = 620/751 lux<br>Halls (general) = 400 lux |

[1]Illuminance levels achieved with the existing installation.

Table 1. Control policies for the lighting system.

### 2.1.2 Ventilation system

Air quality in underground metro stations is usually compromised of rather high $CO_2$ and $PM_{10}$ levels. Although no explicit limits of pollutant levels are set for metro stations, efficient mechanical ventilation is required to maintain good indoor air quality. Acceptable thermal comfort is generally attained as a secondary objective, provided that indoor air quality is achieved. Taking into account that users are only present in metro stations for a few minutes (they normally remain in carriages for longer periods), metro operators are not obliged to adhere to the temperature limits set by thermal comfort standards in regular buildings. In this case, the basic requirement is that the indoor conditions are not too different from those outdoors [19].

During daytime, two identical fans located in the prototype underground station push outside clean air into the station. Their operation is coordinated with two other fans installed in adjacent tunnels, which extract exhausted air to the outside environment. During the night, the fans in the station are turned off, and those in the tunnels are reversed. Consequently, clean outdoor air is injected into the tunnels and exhausted air is forced to pass through the platform area and the corridors to the outside. In the summer, fans run at top speed (1500 rpm) to generate a nominal airflow rate of 62,500 $m^3/h$. The average temperature in the platform area ranges between 28 and 32°C, and the highest temperature peaks are registered late in the afternoon, when tunnel fans reverse their rotation and start injecting air into the platform area, refreshing the tunnels and heating up the platforms until regular daily operation is re-established. Measurement results show that the $CO_2$ level usually ranges between 750 ppm and 1400 ppm in the summer, and is higher during the day. The average level of $PM_{10}$ is 300 $\mu g/m^3$ in the summer, although concentration levels may reach higher peaks during the

early morning or the evening. In winter, since there is no thermal load, the speed of the fans is reduced to control just the air quality, and the airflow generated is halved. In general, the air temperature on the platforms is lower and follows the outdoor trend. Trends in $CO_2$ and $PM_{10}$ concentration levels are quite similar to those registered during the summer period, but the $PM_{10}$ ratio is slightly higher.

Current schedule-based ventilation policies do not consider potential synergies or conflicts from underground airflow dynamics. They may even be counterproductive, because they do not take into account the piston effect of train transit and, more importantly, the chimney effect caused by the depth difference between consecutive underground stations. The weather outside is also a main driver in underground air flow dynamics. Air exchange between the indoor and outdoor environment may be favoured or hindered, depending on the outdoor temperature and the wind direction.

In order to optimize underground ventilation policies, a model predictive control strategy was proposed. The control system adjusts mechanical air supply rates according to an optimal combination of indoor air quality, thermal comfort and energy consumption, taking into account forecasted boundary conditions in any given control cycle (Figure 1).

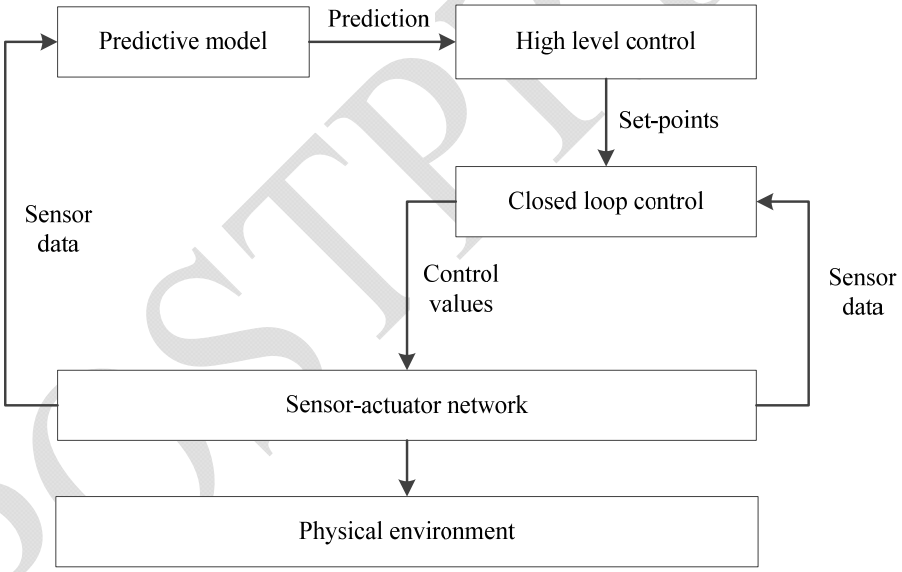


Figure 1. Model predictive control for ventilation.
Source: partially adapted from Ansuini et al. [20].

The energy savings are achieved by minimizing a cost function, calculated as the weighted sum of electricity consumption, thermal comfort and air quality components [21] [eq. 1]. Different sets of weighting coefficients define different control policies, which can be applied in real time without any service interruption (Table 2). Defined control policies include (1) maximum indoor air quality, (2) normal, (3) intermediate, (4) maximum energy saving and (5) maximum thermal comfort. Weighting factors related to air quality and temperature are higher when the control policy prioritizes the indoor air quality or the thermal comfort over the energy saving. Similarly, the

electricity consumption term is weighted over the thermal and air quality terms when seeking maximum energy saving. The intermediate and normal control policies represent a trade-off between the users' comfort and the energy savings but the thermal comfort and air quality weighting factors are slightly higher in the normal policy than in the intermediate policy. The envisaged control policies entail different schedules in which the model predictive control strategy is active. In the maximum indoor air quality policy, the model predictive control works all day (0:00-24:00) whereas in the intermediate control policy, the SEAM4US control only runs when the station is open (5:00-24:00). The normal control policy allows starting the control of the station a certain number of hours before the opening time (P hours before 5:00-24:00). Finally, in both the maximum energy saving control policy and the maximum thermal comfort policy, the model predictive control strategy works from 07:00 to 22:00. Weighting factors were determined empirically according to the requirements specified by the metro station operator but they could be adjusted based on the specific needs.

$$J = \sum_{k=1}^{P} \alpha_{PT} \cdot \left( \frac{\|PElTF1(k) + PElTF2(k)\|}{2 \cdot \widetilde{PT}} \right)^2 + \alpha_{PS} \cdot \left( \frac{\|PElSF1(k) + PElSF2(k)\|}{2 \cdot \widetilde{PS}} \right)^2 + \alpha_{DT} \cdot \left( \frac{\|TOuWS(k) - TemPl3(k)\|}{\widetilde{DT}} \right)^2 + \alpha_{T} \cdot \left( \frac{\left\|\overline{TemPl3} - TemPl3(k)\right\|}{\widetilde{DT}} \right)^2 + \alpha_{AC} \cdot \left( \frac{\left\|\overline{ACOPl3} - ACOPl3(k)\right\|}{\widetilde{AC}} \right)^2 + \alpha_{CO2} \cdot \left( \frac{\|CO2Pl3(k)\|}{\widetilde{CO2}} \right)^2 + \alpha_{PM10} \cdot \left( \frac{\|PM10Pl3(k)\|}{\widetilde{PM10}} \right)^2 + \alpha_{DF} \cdot \left( \frac{\|FreSF1(k) - FreSF1(k-1)\|}{\widetilde{DF}} \right)^2 + \alpha_{DF} \cdot \left( \frac{\|FreSF2(k) - FreSF2(k-1)\|}{\widetilde{DF}} \right)^2 \quad [1]$$

| Control policy | $\alpha_{PT}$ | $\alpha_{PS}$ | $\alpha_{DF}$ | $\alpha_{DT}$ | $\alpha_{T}$ | $\alpha_{AC}$ | $\alpha_{CO2}$ | $\alpha_{PM10}$ |
|---|---|---|---|---|---|---|---|---|
| **Maximum indoor air quality (0:00-24:00)** | 0.204 | 0.204 | 0.153 | 0.051 | 0.051 | 0.051 | 0.051 | 0.051 |
| **Normal (P hours before 5:00-24:00)** | 0.257 | 0.257 | 0.129 | 0.051 | 0.017 | 0.034 | 0.034 | 0.034 |
| **Intermediate (5:00-24:00)** | 0.331 | 0.331 | 0.096 | 0.010 | 0.010 | 0.013 | 0.013 | 0.013 |
| **Maximum energy saving (7:00-22:00)** | 0.331 | 0.331 | 0.096 | 0.010 | 0.010 | 0.013 | 0.013 | 0.013 |
| **Maximum thermal comfort (7:00-22:00)** | 0.092 | 0.010 | 0.000 | 0.134 | 0.531 | 0.004 | 0.036 | 0.008 |

Table 2. Control policies and corresponding weighting factors.

The energy consumption component is estimated from the fan frequencies, and is used to minimize power consumption [eq. 1]. $\alpha_{PT}$ is the weight of the tunnel fan power term, which varies according to a predefined control policy (see Table 2); *PElTF1* and *PElTF2* denote the power absorbed by the tunnel fans and the corresponding values are retrieved from the airflow prediction Bayesian network (see Section 2.2.1); and $\widetilde{PT}$ represents the normalization coefficient corresponding to the typical value of the power absorbed by the tunnel fans. $\alpha_{PS}$ is the weight of the station fan power term, which varies according to a predefined control policy (see Table 2); *PElSF1* and *PElSF2* denote the power absorbed by the station fans and the corresponding values are retrieved from the airflow prediction Bayesian network (see Section 2.2.1); and $\widetilde{PS}$ represents the normalization coefficient corresponding to the typical value of the power absorbed by station fans [eq. 1].

The thermal comfort is assessed using a combination of the difference between the outside and inside temperatures, and the difference between the desired temperature and the actual inside temperature [eq. 1]. In this case, $\alpha_{DT}$ is the weight of the in-out temperature term, which varies according to a predefined control policy (see Table 2); *TOuWS* denotes the temperature of external air and is retrieved from the weather station; *TemPl3* represents the average temperature over all the platform, and the corresponding value is retrieved from the temperature prediction dynamic Bayesian network (see Section 2.2.1); and $\widetilde{DT}$ is the normalization coefficient corresponding to the typical value of the in-out temperature value. The weight of the temperature term varies according to the control policy predefined in Table 2 ($\alpha_T$), and the desired value of the average temperature over all the platform ($\overline{TemPl3}$) is also taken into account [eq. 1].

Finally, the air quality component is estimated through a combination of the difference between actual air exchange and the corresponding reference value, and normalized $CO_2$ and $PM_{10}$ levels [eq. 1]. In this case, $\alpha_{AC}$ is the weight of the air change term that

varies according to the predefined control policy (see Table 2); $\overline{ACOPl3}$ denotes the desired valued for the amount of clean air reaching the platform; *ACOPl3* is the amount of clean air coming from outdoors and entering the platform, and the corresponding value is retrieved from the airflow prediction Bayesian network (see Section 2.2.1); and $\widetilde{AC}$ represents the normalization coefficient corresponding to the typical value of the amount of clean air reaching the platform. The $CO_2$ component includes $\alpha_{CO2}$ (the weight of the $CO_2$ term that varies according to the control policy defined in Table 2); *CO2Pl3* ($CO_2$ concentration in the platform area); and $\widetilde{CO2}$ (normalization coefficient corresponding to the typical value of the $CO_2$ concentration in the platform area). The $PM_{10}$ component considers $\alpha_{PM10}$ (the weight of the $PM_{10}$ term varies according to control policy defined in Table 2); *PM10Pl3* ($PM_{10}$ concentration in the platform area) and $\widetilde{PM10}$ (the normalization coefficient corresponding to the typical value of the $PM_{10}$ concentration in the platform area) [eq. 1].

An additional term is used to penalize high frequency variations. In this case, $\alpha_{DF}$ is the weight of the frequency variation term that fluctuates according to the predefined control policy (see Table 2); *FreSF1* and *FreSF2* denote the frequency of each station fan and are the output for the controller; and $\widetilde{DF}$ represents the normalization coefficient corresponding to the typical value of the frequency of each station fan [eq. 1].

In any case, minimum indoor air quality and thermal comfort levels must be granted and thus four control rules are defined: (1) the indoor temperature (*TemPl3*) must be lower than a maximum threshold [eq. 2], (2) the air exchange level in the platform area *(ACOPl3)* must be greater than a minimum threshold modulated by the actual number of people on the platform (*NPePl3*) in relation to the typical value of people on the platform ($\widetilde{NPePl3}$) [eq. 3], (3) the difference between the inside $CO_2$ level *(CO2Pl3)* and the outside $CO_2$ level *(CO2Out)* must be lower than a maximum level [eq. 4] and (4) the $PM_{10}$ level ($PM10Pl3$) must be lower than a maximum threshold [eq. 5]. An additional constraint related to the operation of station fans was also included [eq. 6]. Configurations that violate these constraints are rejected. Reference values are based either on regulations (when available) or on specific operational policies set by the metro operator (Table 3).

$$TemPl3(k) < TemPl3_{Max} \quad [2]$$

$$ACOPl3(k) > \frac{NPePl3}{\widetilde{NPePl3}} \cdot ACOPl3_{Min} \quad [3]$$

$$CO2Pl3(k) - CO2Out(k) < DCO2Pl3_{Max} \quad [4]$$

$$PM10Pl3(k) < PM10Pl3_{Max} \quad [5]$$

$$FreSF_{Min} < FreSF1(k) = FreSF2(k) < FreSF_{Max} \quad [6]$$

| Parameter | Reference value |
|---|---|
| Maximum temperature for the platform ($TemPl3_{Max}$) [ºC] | 31.00 |
| Minimum air exchange level in the platform area ($ACOPl3_{Min}$) [kg/s] | 3.93 |
| Difference between inside and outside $CO_2$ levels ($DCO2Pl3_{Max}$) [ppm] | 370.00 |
| Maximum $PM_{10}$ concentration level in the platform area ($PM10Pl3_{Max}$) [µg/m$^3$] | 140.00 |
| Minimum frequency of station fans ($FreSF_{Min}$) [Hz] | 0 |
| Maximum frequency of station fans ($FreSF_{Max}$) [Hz] | 50 |

Table 3. Reference values setting minimum indoor air quality and thermal comfort levels.

For each control step, the system generates alternative configurations, which are ranked according to the value of the cost function. The solution that results in the lowest cost is selected. According to current schedule-based ventilation policies, in the summer the fans are operated at top speed (+50Hz). However, in the case of a summer's day with a south wind, the model predictive control found that station fans should be operated in reverse (-50 Hz), in order to achieve improved indoor conditions. Similarly, in the case of a winter's day with a north wind, the model predictive control found that station fans could be stopped instead of running at the pre-defined frequency of +25 Hz. In this case, tunnel fans and the wind through the corridors provide enough air exchange, and thus both $CO_2$ and $PM_{10}$ concentration levels are acceptable and the temperature is pleasant.

### 2.1.3 Escalators

Passenger transfer systems move passengers out of the station, taking them from underground to street level and vice versa. Besides having two hydraulic, low consumption electric elevators, the station is also equipped with two escalators connecting the halls with street level, and covering a total distance of 10.49 m. Both escalators have automatic start-stop operation and remote control activation. Escalators in the underground station travel at a nominal speed of 0.5 m/s, which is fast enough to provide rapid displacement whilst maintaining comfort and safety (transport mode). Escalators operate at 0.2 m/s when they are empty (stand-by mode).

In order to enhance the energy efficiency of the underground station, the system introduces new speeds within the escalators' operational range. When there are no passengers, the escalator is stopped using a radar sensor. When there is no risk of generating queues, the nominal speed (0.5 m/s) is reduced to a lower speed (0.4 m/s) that is technologically capable of moving passengers, but consumes less energy. Therefore, the main driver of escalator control is passenger transit. Upwards escalators that are closer to the platform are affected by train arrivals, and thus their transport speed hint is based on the platform's occupancy level. Occupancy peaks are dynamically isolated on a daily basis and the threshold, which can be variable, is set to

65% of the maximum foreseen occupancy. In order to be effective, decisions about transport speed hints are maintained at least for the time it takes for people to travel from platform to escalators. Table 4 reports the adopted transport and standby speeds, depending on the occupancy level and the existing active control. Due to escalator safety standards, the speed cannot be changed whilst passengers are in transit. In any case, the speed is only changed when the escalators' photocells detect that nobody is using them.

| | **Speed [m/s]** |
|---|---|
| **Transport mode** | |
| Occupancy > threshold or the occupancy is not available | 0.5 |
| Occupancy ≤ threshold | 0.4 |
| **Standby mode** | |
| Radar switch OFF | 0.2 |
| Radar switch ON | 0.0 |

Table 4. Control policies for escalators.

## 2.2 DEVELOPMENT OF ENVIRONMENTAL AND OCCUPANCY MODELS

### 2.2.1 Environmental model

The environmental modelling of the entire metro station required the development of an ad hoc methodological framework including three main steps: (1) qualitative modelling, (2) quantitative modelling and (3) model reduction.

During the first step and in order to investigate the airflow dynamics of the underground station, several computational fluid dynamic (CFD) models were developed that encompassed different spatial scales (urban canyon models, overall indoor airflow models and local indoor airflow models). Simulations were useful to impose external weather dynamics' boundary conditions on the whole building model, by computing wind pressure coefficients at the station entrances. Simulations also supported the sensor network design by analysing ventilation patterns at different points of the station. Models were validated through an on-site measurement campaign using a weather station placed on top of one of the entrances [22]. Although the CFD modelling provided a qualitative insight into the station's behaviour, it did not offer enough flexibility to be included in a complex control algorithm [20].

During the second step, a lumped parameter model of the entire station was developed using Dymola [23], a commercial simulation environment widely used to model complex physical systems. Dymola is based on Modelica [24], an non-proprietary, object-oriented, equation based modelling language. At the top level, the model structure reflected the station topology. All the spaces were represented separately (platform, hall, corridor and staff rooms), and connected according to the real station.

Each space had a core component modelling the heat and mass transfer processes occurring in its environment. This basic component was then connected to a set of other components modelling the relevant dynamics of underground subway spaces (pollutant sources, internal gains, thermal exchange with the ground, airflow resistances and pressure drops due to buoyancy). At the top level, the Dymola model also included other components modelling the main disturbance processes occurring in a subway station: weather, trains and people. Specific wind pressure coefficients retrieved from CFD models were also included. Evidence-based calibration was performed in accordance to the methodology suggested by Raftery et al. [25]. As described in Giretti et al. [26], a multi-stage approach was adopted including (1) sensitivity analysis, (2) preliminary raw calibration and (3) evidence-based calibration. The sensitivity analysis allowed the identification of the most influencing processes and parameters. The raw calibration phase used both real-time monitoring data and measures retrieved from environmental surveys, leading to an overall revision of the model. Finally, the evidence-based calibration allowed refining the role of several critical parameters. Figure 2 shows a high similarity between the on-site data collected by four temperature sensors located on the platform, and the simulated temperature for the whole platform zone. Both the monthly or hourly normalized mean bias error (NMBE) and the coefficient of variance of root mean square error (CV-RMSE) were found to be much lower than the recommendations set up by the ASHRAE guideline 14 [27] (NMBE: 10%; CV-RMSE: 30%). The slight mismatch observed during the second part of the day can be attributed to the considerable thermal gain introduced by train air conditioning, whose set-up may vary from train to train and which is difficult to rule out. Figure 3 compares the simulated and measured power consumption of station fans. In this case, calibration indexes calculated according to the ASHRAE guideline 14 [27] also showed good accuracy (NMBE: 7.9%; CV-RMSE: 10.88%).

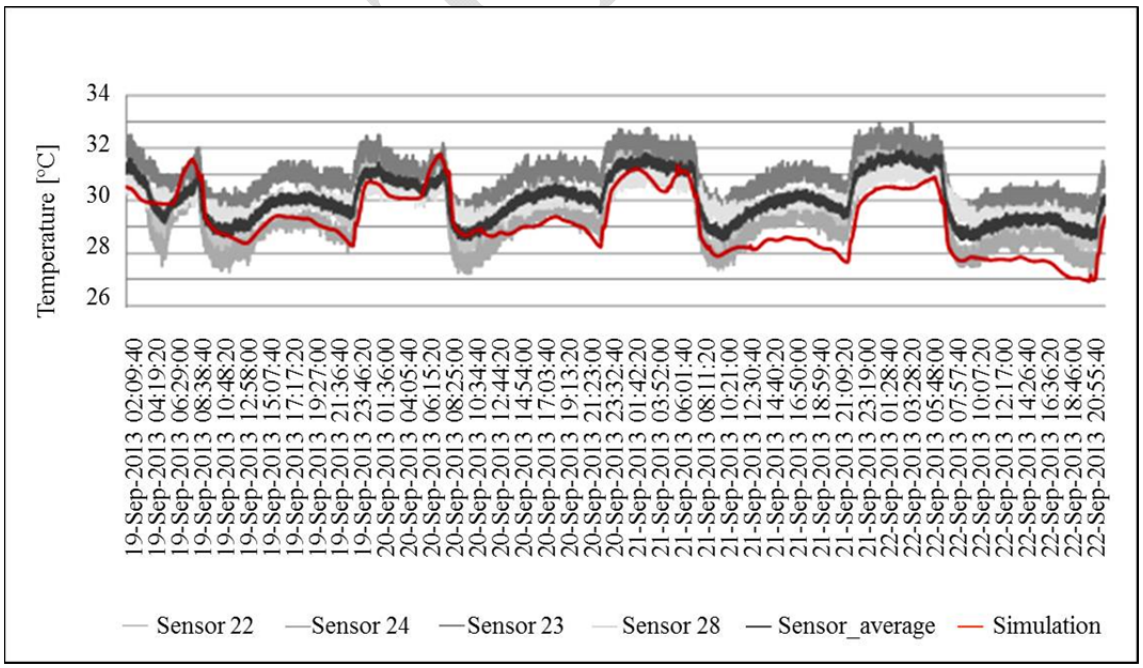


Figure 2. Comparison of simulated and measured air temperature in the platform area.

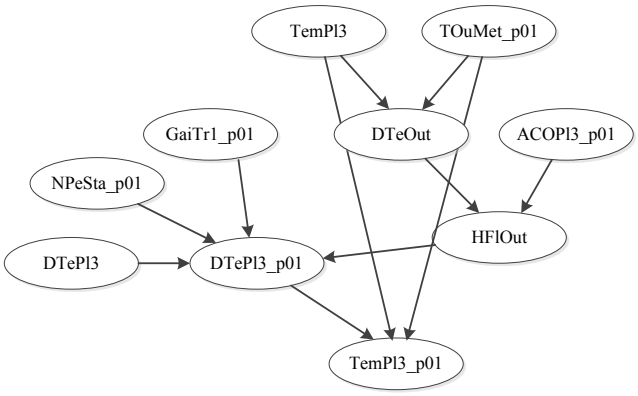


Figure 3. Structure of the temperature prediction dynamic Bayesian network. Source: Carbonari et al. [21].

Taking into account that running the station model in real-time would be computationally unfeasible, it was reduced by adopting the approach of dynamic Bayesian networks. A large set of control cases generated by the station model were analysed to identify the minimum set of parameters necessary for effective control of target performances. Hierarchical clustering and k-means partitioning algorithms were used to identify redundant parameters [28]. After an iterative process, only those parameters showing the strongest dependence relationships were kept [21]. The statistical clustering process suggested the separation of the heat transfer and fluid dynamics physics. Consequently, two Bayesian network models were developed (Figure 4 and 5). According to Figure 4, the temperature of the platform in the next step (*TemPl3_p01*) can be predicted taking into account the forecasted number of people in the station at the next step (*NPeSta_p01*), the forecasted train thermal gains (*GaiTr_p01*), current platform temperature (*TemPl3*), forecasted outdoor temperature (*TOuMet_p01*), forecasted air changes per hour (*ACOPl3_p01*) and deviation of temperature from the past time step (*DTePl3*). According to Figure 5, the air flow rates expected in the corridors leading to the platform (*AFlCNl_p01*, *AFlCNop_p01*, *AFlCNq_p01*, *AFlSlb_p01*) and the power consumption of both station and tunnel fans (*PElSF1*, *PElTF1*, *PElTF2*) can be predicted taking into account the forecasted frequencies of fans in the stations and tunnels at the next time step (*DFreTF1_p01*, *DFreTF2_p01*, *DFreSF1_p01*), forecasted train thermal gains (*GaiTr_p01*), forecasted wind direction and speed (*WiDMet_p01*, *WiSMet_p01*), outdoor temperature (*TOuMet_p01*) and current platform temperature (*TemPl3*). The overall air change over the platform (*ACOPl3*) is calculated taking into account estimated air flow rates (*AFlCNl_p01*, *AFlCNop_p01*, *AFlCNq_p01*, *AFlSlb_p01*), and linking this network with the temperature prediction dynamic Bayesian network (Figure 4). In order to assess the approximation introduced by the model reduction process, Bayesian networks were validated by comparing the results with data computed by the lumped parameter model. As shown in Figure 6, the prediction accuracy achieved by the reduced model was found to be good enough to obtain reliable control of the station.

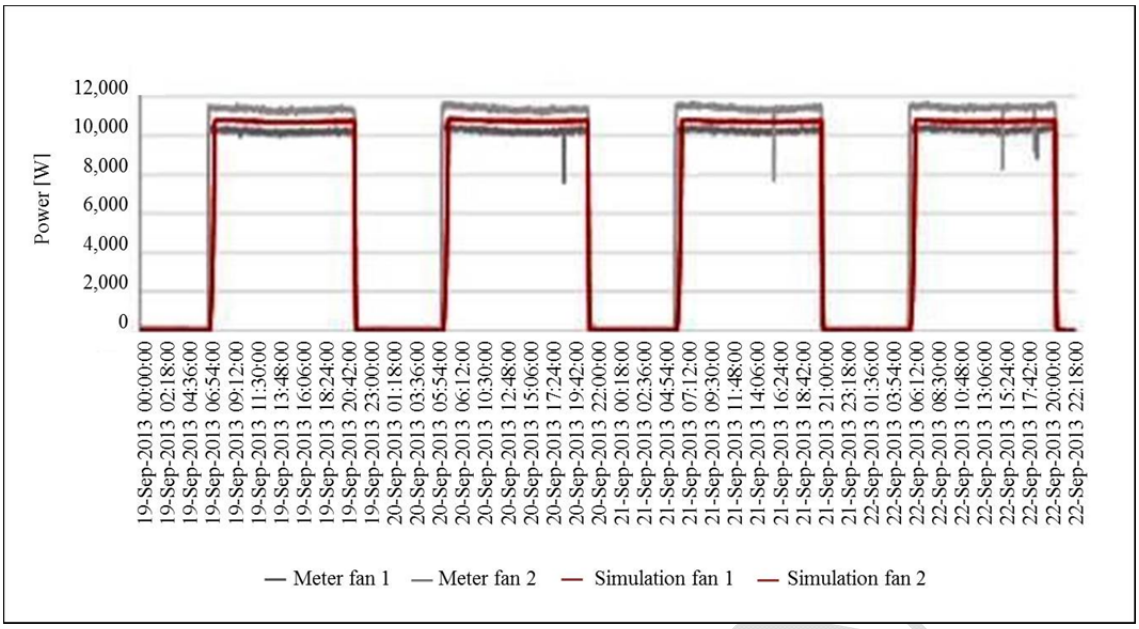


Figure 4. Comparison of simulated and measured power consumption of station fans.

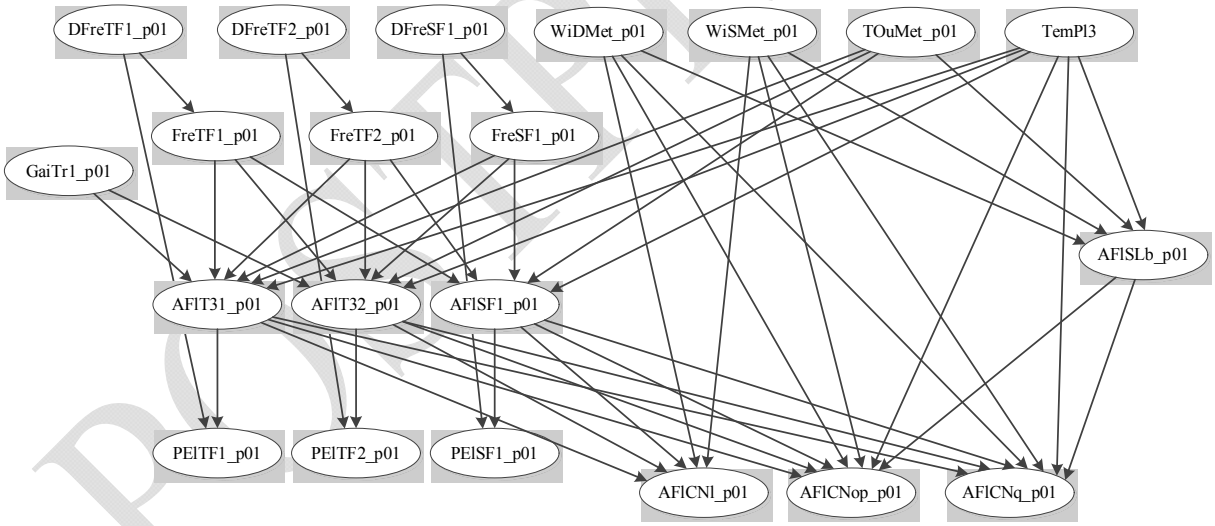


Figure 5. Structure of the airflow prediction Bayesian network.
Source: Carbonari et al. [21].

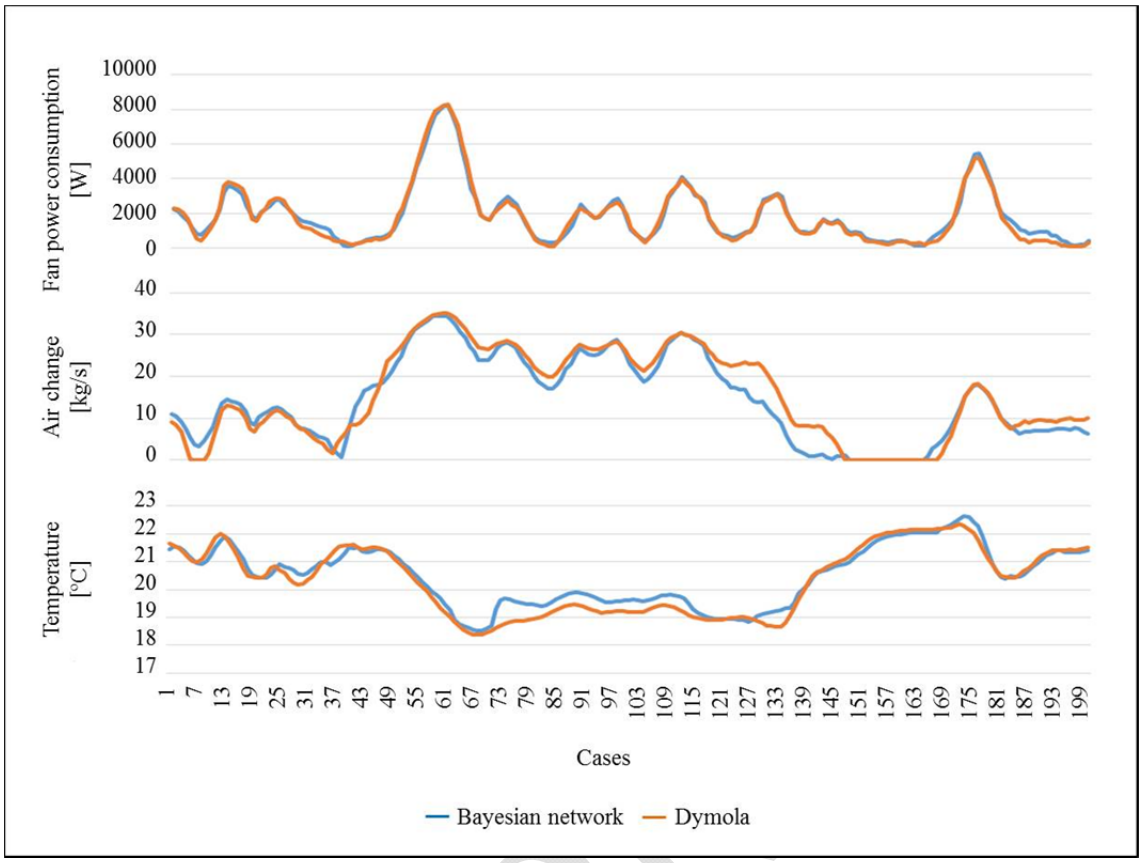


Figure 6. Comparison between the simulated and the estimated fan power consumption (*PElSF1_p01*), air change (*ACO_p01*) and platform temperature (*TemPl3_p01*).

### 2.2.2 Occupancy model

Monitoring the density of passengers and their flow patterns provides valuable information to link occupancy behaviour to energy consumption. The model is exclusively based on video streams of the existing CCTV surveillance system. First of all, in order to avoid feeding the algorithm with noise from uninteresting areas of the frame, regions of interests and perspectives are established for each camera (Image 1 in Figure 7). Secondly, the background frame is identified by detecting the pixels that remain unchanged during several temporal sections (Image 2 in Figure 7). Thirdly, the foreground mask is created by extracting the foreground and removing the noise through a simple erosion algorithm (Image 3 in Figure 7). Concurrently, edges of the foreground image are detected and extracted. The last step of the crowd density detection algorithm consists in combining the last image with the foreground mask. Results are refined by dilating and then eroding the segmented blobs of people (Image 4 in Figure 7). Finally, the size of the blobs is related to the actual number of people in them, and crowd density estimations from individual cameras are aggregated according to the pre-defined zones. The algorithm can estimate the crowd with less than 20% error, which means that, in general, the density monitored is within a ±2 people range of the actual figure. In case of low density of people, the error was found to tend to zero whereas more people highly overlapped involved higher errors. However it must be taken into account that this is not critical as the same control policy applies above a given occupancy threshold. Taking into account that anomalous situations such as a

scratch on the camera could compromise the robustness of the CCTV-based crowd density estimation algorithm, a buffer time of a few minutes ensures that an absolutely motionless object becomes part of the background and thus is ignored by the algorithm.

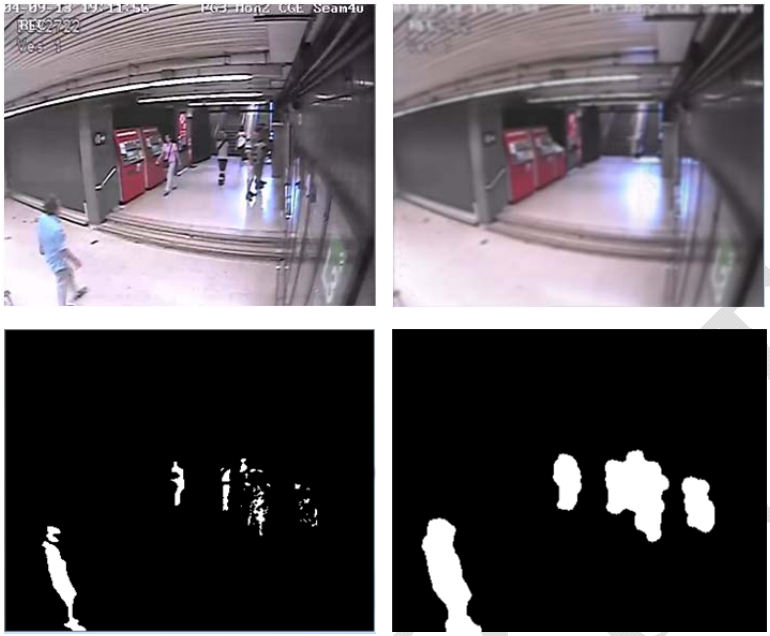

Figure 7. Main steps of the crowd estimation algorithm.

In order to predict the crowd density, the algorithm uses the sequence alignment approach, and compares two context sequences. The first sequence represents the current sensed density of a given location called observation. The second sequence represents the history of passenger density in the same location. The matching process identifies the pattern in the history that is most similar to the current observation pattern. Subsequently, the context that follows the identified pattern is predicted (Figure 8).

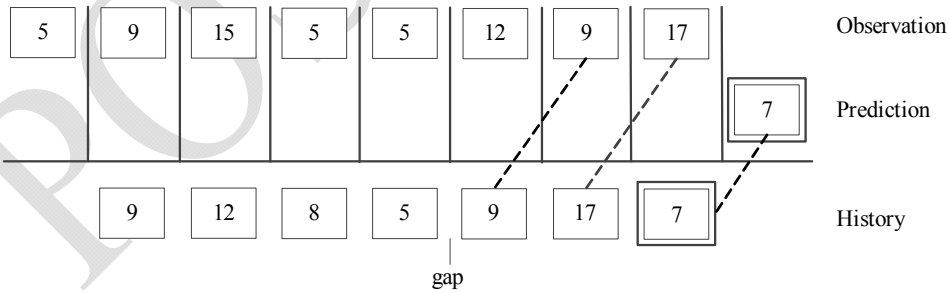


Figure 8. Example of the alignment approach.
Source: partially adapted from Sigg [29].

Prediction accuracy was assessed for seven days in twelve locations. The average prediction error (the difference between the predicted and actual number of passengers) was found to be -0.06. The prediction error for locations with low occupancy was found to be close to zero, while the prediction error was found to increase for locations with a higher average number of passengers, and therefore greater passenger fluctuation.

## 2.3. INTEGRATION OF THE SYSTEM

The SEAM4US control system was integrated into the existing metro operator's control system, taking into account the metro operator's safety requirements. SEAM4US control is only effective within the service mode and under normal conditions if this is stated by the operator's control center. When the system is in maintenance mode or normal mode and an emergency occurs, the default control mode prevails (Figure 9).

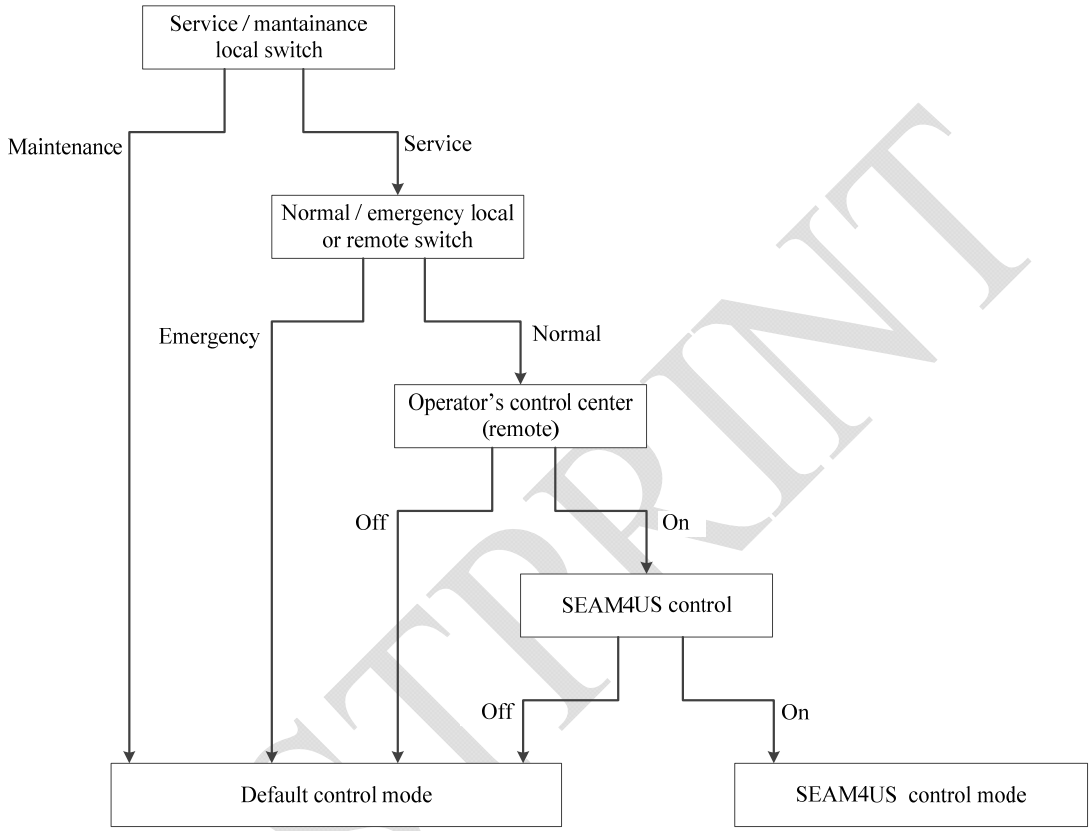


Figure 9. Hierarchy of control modes.

## 2.4. PILOT IMPLEMENTATION

The intelligent energy management system was built upon the existing infrastructure of the pilot underground station. Several control components were installed to act on existing lighting, ventilation, and escalators. In accordance with the envisaged control policies, several measurement and prediction inputs were also needed. Lighting and escalator control policies demanded real-time data on crowd density and energy consumption, whereas ventilation control policies required both environmental and energy consumption data. Thus, a monitoring network was implemented that created almost real-time awareness of these key aspects. Finally, backend equipment was installed to remotely manage and support the monitoring network and the control components.

### 2.4.1 Lighting pilot

The lighting pilot involved three areas of the prototype station, including meaningful portions of three typical station spaces (platform, hall and stairs). Existing lighting fixtures were upgraded to support a digital addressable lighting interface (DALI) controller. Corresponding compatible ballasts were also installed. A wired connection was used between ballasts and a DALI gateway (placed inside a cabinet installed in the low voltage room). The DALI gateway could be accessed through a web browser or customized software, using a RESTful API. The SEAM4US server communicated with the DALI gateway through the HTTP protocol. The connection to the SEAM4US server was achieved through a wired Ethernet connection, and thus the Wi-Fi functionality of the DALI gateway was disabled. The SEAM4US system included a software component providing methods to access the gateway's functionality, in particular to dim the lights by zone, as required by the controller. The SEAM4US control could also be disconnected, if needed, through a switch placed on the front door of the cabinet to restore the original functionalities of the system.

### 2.4.2 Ventilation pilot

Commands sent by the SEAM4US server were transferred to the ventilation system through new PLCs deployed in parallel with the existing ones. PLCs modulated the fans' speed by controlling the corresponding variable frequency drives. In order to provide feedback to the control system, each fan was equipped with an anemometer measuring air speed. For the same reason, the direction and speed of the existing station fans could be retrieved through the same PLC, as well as the status of the variable frequency drives. All this additional hardware was installed in a new cabinet next to the existing ones in the ventilation room. Dedicated control logic ensured that the operation of this safety-critical system was unimpeded even in critical situations (i.e. extraction of smoke in case of fire, failure of the SEAM4US system, etc.). A dedicated switching logic with relays providing galvanic isolation between different control signals was installed, allowing explicit change between the default control and the SEAM4US control. The switching logic could also be controlled by the operator's control center or locally by maintenance operators using a push button placed on the front of the cabinet.

### 2.4.3 Escalator pilot

In order to make sure that the escalator only started to operate when people needed to be conveyed, a radar sensor was installed. One additional input indicating the desired speed was added to the escalator controller. If the radar sensor indicated that there are no users on the escalator, the controller allowed the system to change the rated speed to between 0.4 m/s and 0.5 m/s. In order to indicate the state of the escalator to the SEAM4US system, four digital outputs were added to the escalator controller. One of the outputs indicated the current speed set in the escalator: stopped (0 m/s), standby (0.2 m/s), low speed (0.4 m/s) or full speed (0.5 m/s). The variable frequency drive of the escalator was also reprogrammed to support the new transport speed of 0.4 m/s. A dedicated programmable logic controller (PLC) was installed to interface the escalator control with the SEAM4US server. This PLC provided one digital output and four digital inputs, corresponding to the current speed of the escalator, and it was connected to the existing escalator PLC through one relay for each signal. The SEAM4US control could also be locally disconnected.

### 2.4.4 Environmental, occupancy and energy consumption monitoring network

In order to capture the station's ambient data, an extensive set of supported sensors was deployed in the station. Sensors were selected taking into account several competing features, such as accuracy, resolution, range, stability, maintainability, energy consumption, operating voltage, physical dimensions and cost (Table 5). Wireless sensing was considered suitable not only because of the temporary character of the pilot implementation and non-availability of communication and power infrastructure, but also to reduce installation costs. The wireless sensor network was designed to optimize the maintenance costs associated with battery replacement and network management. In addition, self-diagnostics and self-configuration capabilities ensured correct operation without human intervention. Sensor nodes contained multiple sensors measuring environmental data. This information was communicated through ZigBee radio with other nodes, including the gateway node, providing multi-hop capability. The gateway node communicated with the WSN gateway (a computer hosting local database server software and providing interfaces to the sensor network's management user interface) through RS485. The weather station component sent the measurement data to the gateway server through an RS485 link. The sensor network deployment was validated with several on-site surveys. Calibration surveys mainly aimed to eliminate the effects of noisy inputs, due to the installation of the sensors (i.e. heat caused by lamps, turbulent flow, etc.). Although accurate absolute measurements were not required by the implemented control techniques (control algorithms use relative measurement values instead of absolute values), sensor biases were also determined through on-site surveys.

| Sensor type | Number of units | Accuracy | Resolution | Range |
|---|---|---|---|---|
| **Air temperature sensor** | 27 | ±0.50°C (typical) | 0.25°C | −40°C to +125°C |
| **Surface temperature** | | ±0.50°C (typical) | 0.25°C | −40°C to +125°C |
| **Relative humidity sensor** | 1 | ±5% (total error band) | 0.04% | 0% to 100% |
| **Integrated air temperature** | | ±1°C (maximum) | 0.025°C | +5°C to +50°C |
| **Air pressure sensor** | 28 | 100 Pa (typical) | 1 Pa | 300 to 1100 hPa |
| **Integrated air temperature** | | ±0.5°C (typical) | 0.1°C | −40ºC to +85.0°C |
| **Differential air pressure sensor** | 2 | 1.5 % (measured value) | 0.04 Pa | 0 to 100 Pa |
| **Integrated air temperature** | | 2.0°C (typical) | 0.1°C | 0 to 70°C |
| **High speed anemometer** [1] | 12 | ±2.0% (typical) | 0.1 m/s | 0.4 to 30.0 m/s |
| **Low speed anemometer** | 2 | ±0.300 m/s (typical) | 0.001 m/s | 0 to 5 m/s |
| **Pyranometer** | 1 | ±20 W/m² | 2 W/m² | 0 to 2000 W/m² |
| **Indoor $CO_2$** | 2 | ±50 ppm ± 3% (measured value) | 1 ppm | 0 to 5000 ppm |
| **Outdoor $CO_2$** | 1 | ±50 ppm ± 3% (measured value) | 1 ppm | 0 to 2000 ppm |
| **Indoor $PM_{10}$** [2] | 2 | ±500 pcs/283ml (typical) | 10 pcs/283 ml | 0 to 20000 pcs/283ml |
| **Outdoor $PM_{10}$** | 1 | ±0.1 mg/m$^3$ (maximum) | 0.0002 mg/m$^3$ | 0 to 0.5 mg/m$^3$ |
| **Supported weather station** | 1 | | | |

| Sensor type | Number of units | Accuracy | Resolution | Range |
|---|---|---|---|---|
| **Air pressure** | | ±0.5 hPa (typical) | 0.1 hPa | 600 to 1100 hPa |
| **Air temperature** | | ±0.3°C | 0.1°C | -52°C to +60°C |
| **Relative humidity** | | ±3% (typical) | 0.1% | 0% to 100% |
| **Rain accumulation** | | 5% (measured value) | 0.01 mm | n.a. |
| **Rain duration** | | 10 s | 10 s | n.a. |
| **Wind speed** | | ±0.3 m/s or ±3% (measured value) | 0.1 m/s | 0 to 60 m/s |
| **Wind direction** | | ±3° | 1° | 0 to 360° |

[1] Modified to enable flow direction measurement.

[2] Particle size over 0.5 μm.

Table 5. Main characteristics of the sensors installed in the underground pilot station for monitoring environmental data. Source: adapted from VTT [25].

The occupancy detection subsystem was relayed on the existing closed-circuit television (CCTV) infrastructure. A video recorder combined the information gathered by 20 selected cameras distributed evenly throughout the station into a single video stream. This video stream was later processed by a robust video-processing algorithm, running on a desktop computer. The privacy of passengers was protected by performing all processing locally on-the-fly with no computer storage, filtering the image data to avoid recognisability of individuals, and transmitting only density levels in terms of integer numbers.

Detailed data about the energy consumption of individual subsystems in the underground stations were useful for generating energy consumption baselines and giving real-time feedback on the energy management system performance. For fairly stable loads such as lighting or ventilation systems, a single smart meter measuring multiple power lines was used. This scalable solution enabled the wireless transfer of measurement data, but with reduced monitoring frequency. For highly variable loads such as escalators, a high-performance solution measured with higher frequency, but fewer power lines at once. Measurement data were transferred through RS485 and Modbus/TCP protocols. In both cases, monitoring devices were based on off-the-shelf solutions (Table 6).

| Sensor type | Number of units | Accuracy | Resolution | Range |
|---|---|---|---|---|
| **Fan sensor** | 2 | 3% | 0.01m/s | 1.25 to 75 m/s |
| **High accuracy smart meter** | 2 | 0.2% current and voltage<br>0.5% power and power factor<br>0.1% frequency | 0.1 A | 0 to 15 A |
| **Low accuracy smart meter** | 15 | 1% | 0.1 A | 0.75 to 14.25 A |

Table 6. Main characteristics of the sensors installed in the underground pilot station for monitoring energy consumption.

### 2.4.5 Backend equipment

The backend equipment included a centralized server and backup hard drive disk providing central processing and storage capacity to the SEAM4US system. Due to public transport operators' strict security policy, this equipment could not be cloud-based and had to be located at the operator's control center. For security reasons and to reduce network traffic, proxy servers (gateways) were used locally to pre-process raw data.

## 3. VALIDATION AND DISCUSSION OF THE RESULTS

The International Performance Measurement and Verification Protocol [31] was used to verify and validate the SEAM4US system from a technical and functional perspective.

Implemented control policies were validated separately, taking into account that the subsystems (lighting, escalators and ventilation) were all powered with electricity, but did not overlap and can be monitored individually.

### 3.1 Lighting system

Taking into account that lighting system savings were mainly driven by the passenger flow rate, and in order to assess the lighting control system performance, a comparison between recorded occupancy and the corresponding lighting level was conducted. Figure 10 corroborates an inverse relation between the occupancy and the lighting level. Energy savings achieved with the lighting control system were determined by partial field measurement [31] and are reported in Table 7. Energy savings were calculated taking into account the average power baseline and the measured average power in the reporting period for both the platform and hall 0, and considering the fraction of controlled lamps. Saving errors were calculated according to the error propagation rules stated in the International Performance Measurement and Verification Protocol [31]. Taking into account that the platform consumes 34% of the installed power and the halls and the corridors consume the remaining 66%, energy saving values were extrapolated for the entire station, to obtain an average saving of 24.1% ± 1.9%.

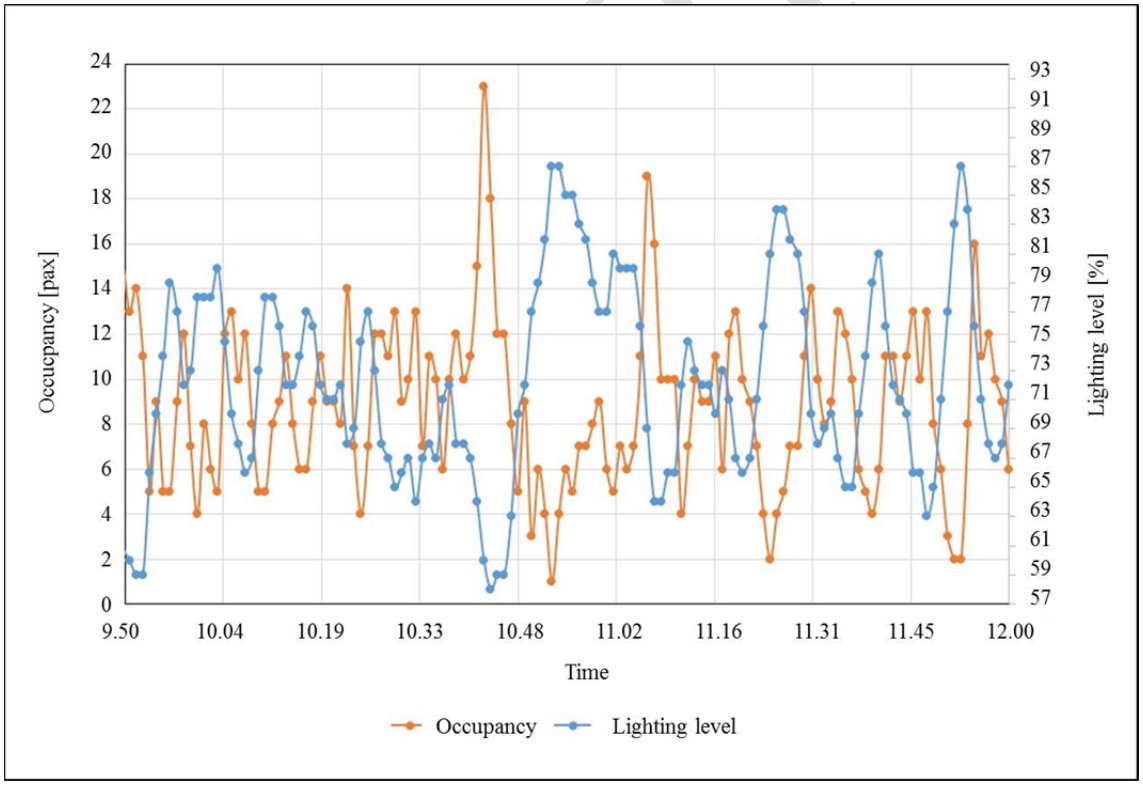


Figure 10. Monitored dynamic trends of occupancy and lighting level for a time period of two hours.

| Areas of lighting pilot | Average power baseline [VA] | Average power with the implemented control policy [VA] | Fraction of controlled lamps [%] | Energy savings [%] |
|---|---|---|---|---|
| Platform | 4,442 ± 5 | 4,393 ± 1 | 7.0 | 15.8 ± 1.7 |
| Hall 0 | 5,701 ± 16 | 5,536 ± 3 | 10.2 | 28.3 ± 2.8 |

Table 7. Energy consumption measured on-site before and after implementing lighting control policies and the corresponding energy savings.

### 3.2 Ventilation system

The assessment of the ventilation control system's performance was challenging due to the multiplicity of external influencing factors that have seasonal dynamics (including temperature, wind speed and direction, and indoor temperature). The representativeness of the monitoring periods for the purpose of the energy savings calculations is compromised, even if it is extended to a whole year. In addition, considerable variations in weather conditions are now much more frequent than in the past, and may occur even within two subsequent weeks. The effects of complex weather variations cannot be compensated, except by modelling the weather dynamics and the building response. Therefore, and according to the International Performance Measurement and Verification Protocol [31], calibrated simulation was used to validate the energy savings achieved with the ventilation control system. The building calibrated simulation model developed within the project for the purpose of the model predictive control of the fan was used to estimate the energy consumed by the ventilation system before and after implementing control policies. Simulations were marginally affected by the model calibration error, since the calibration error equally affects both baseline and controlled reporting period figures. In addition, the simulations avoided any seasonal effect by using standardized and representative weather files [32].

Ventilation control policies were found to achieve significant energy savings (Table 8), without penalizing environmental comfort (Table 9). Reduced speed lowers the saving potential during the autumn and winter, whereas very hot days require high ventilation rates, and thus higher absolute savings can be achieved (Table 8). The relative amplitude of the saving percentage intervals depends on the influence that the weather and operating conditions have on the control range. A temporary decrease in comfort parameters in relation to the baseline is allowed, as long as the levels do not surpass the comfort thresholds. However, and in the worst case (the spring), 75% of differences between baseline and controlled temperatures lie within an interval of ± 0.5°C (Table 9).

| Season | Number of months | Average energy consumption baseline [KWh/week] | Average energy consumption with the implemented control policy [KWh/week] | Energy savings [%] |
|---|---|---|---|---|
| Spring | 3 | 1,595.84 | 1,072.27 | 32.81 ± 1.98 |
| Summer | 4 | 1,541.03 | 1,030.01 | 33.16 ± 1.10 |
| Autumn | 2 | 370.57 | 310.28 | 16.27 ± 5.17 |
| Winter | 3 | 370.33 | 309.93 | 16.31 ± 4.94 |
| Weighted average | - | 1,066.98 | 740.60 | 30.59 ± 2.00 |

Table 8. Simulated energy consumption before and after implementing ventilation control policies and the corresponding energy savings.

| Season | Platform temperature [°C] | | $CO_2$ [ppm] | | $PM_{10}$ [µg/m$^3$] | |
|---|---|---|---|---|---|---|
| | Mean difference | Standard Deviation | Mean difference | Standard Deviation | Mean difference | Standard Deviation |
| Spring | -0.46 | 0.25 | -25.02 | 46.94 | -5.70 | 58.22 |
| Summer | -0.17 | 0.13 | -61.15 | 57.80 | -17.96 | 56.39 |
| Autumn | 0.36 | 0.18 | 34.86 | 60.58 | 7.94 | 14.20 |
| Winter | 0.10 | 0.10 | 13.61 | 42.78 | 4.16 | 10.81 |

Table 9. Mean difference and standard deviation of the main comfort parameters for each season.

In order to provide further evidence, a second set of analyses was carried out based on measured performance data. The objective of this second analysis was to demonstrate that the estimations provided by the calibrated simulation model were in the range of what can be effectively measured by the monitoring system. Measured performance data were recorded during the months of September and October 2014, and the SEAM4US system adopted the same control policy (maximum thermal comfort policy) used in the calibrated simulation. Table 10 reports the calculated savings for the reporting period represented by the two aforementioned months. The consumption baseline was defined as the average power consumed between the middle of May and the first week of July 2014 (summer operation mode). Both the consumption baseline and the average power absorbed in the reporting period were calculated through the measurements recorded by means of the smart meters deployed in the underground pilot station. The expanded uncertainties were calculated according to JCGM 100:2008 [33]. Errors were calculated according to the error propagation rules stated by the

International Performance Measurement and Verification Protocol [31]. Results of the two analyses differ because the weather conditions stated in the weather file were inevitably different from what effectively occurred during the monitored months.

| Months | Average power baseline [VA] | Average power in the reporting period [VA] | Energy savings [%] |
|---|---|---|---|
| September | 23,247 ± 121 | 15,894 ± 915 | 31.6 ± 4.0 |
| October | 23,247 ± 121 | 13,368 ± 860 | 42.5 ± 3.7 |
| Average | 23,247 ± 121 | 15,031 ± 701 | 35.3 ± 3.1 |

Table 10. Measured consumption and savings obtained in the ventilation pilot.

### 3.3 Escalators

Taking into account that an escalator's operating conditions are mainly determined by the occupancy and the escalator's speed, the proper behaviour of the escalator's control system was assessed through (1) the congruity between the predicted occupancy and the signal sent to the escalator and (2) the consistency between the hint sent and the actual speed assumed by the escalator. Figure 11 shows the recorded occupancy and the speed hint sent by the control system for a time period of one hour. In this case and according to Table 4, the speed hint was set to be reduced from 0.5 to 0.4 m/s when the occupancy was under a pre-defined threshold of 15 people. Thus, it can be concluded that the speed hint was consistent with the occupancy threshold 76% of the time (Figure 11). Figure 12 shows the correlation between recorded speed hints and the actual escalator's speed for a time period of one hour, and allows us to conclude that the escalator's speed was actually adjusted to the value suggested by the controller 75% of the time. In this case, and according to the International Performance Measurement and Verification Protocol [31], savings were determined through simulation of the energy use, because the escalator's variable frequency drive efficiency curve showed a severe energy efficiency loss at reduced speeds. However, taking into account that the feasibility of the suggested approach (energy savings through speed modulation) is already well-documented in the existing literature [34, 35] and is rapidly hitting the market [35], a model was calibrated to replicate exactly the measured escalator power and efficiency curves. Consequently, and in accordance with the International Performance Measurement and Verification Protocol [31], the energy savings were estimated by simulating the model on the real data recorded by the occupancy network. The energy savings achievable by implementing the escalator's control policy were estimated to be 8.5% ± 1.9%.

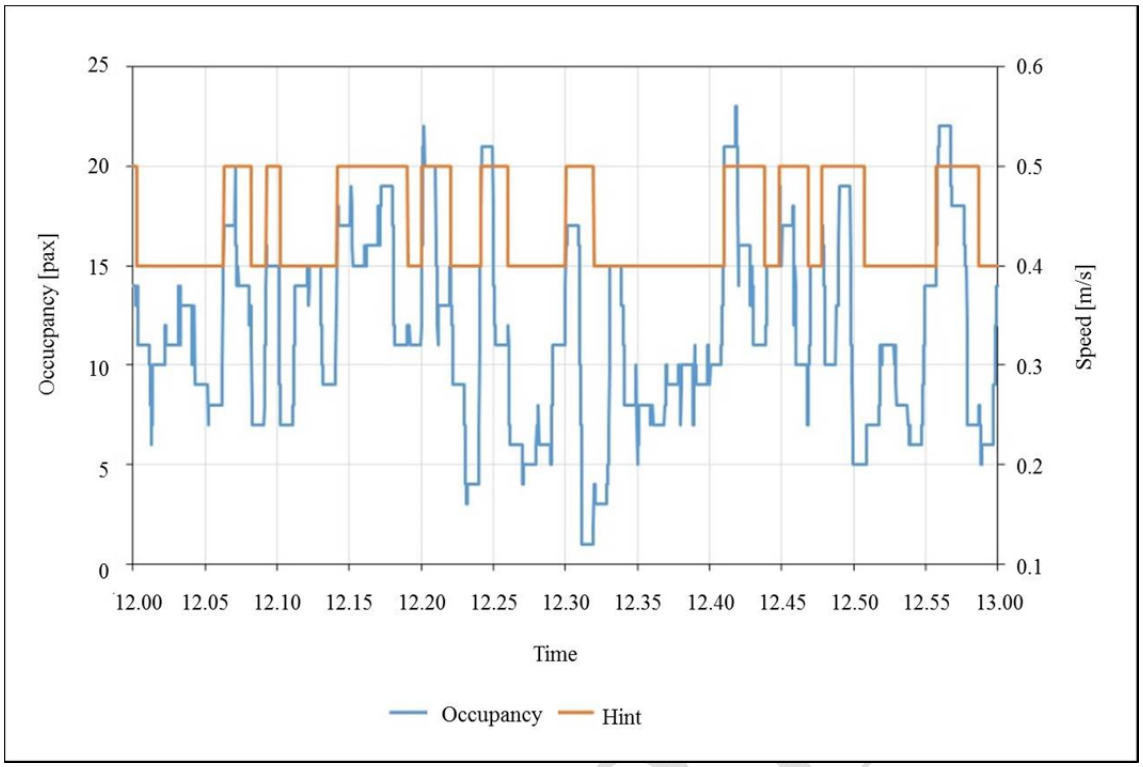


Figure 11. Monitored dynamic trends of occupancy and speed hint sent by the control system for a time period of one hour.

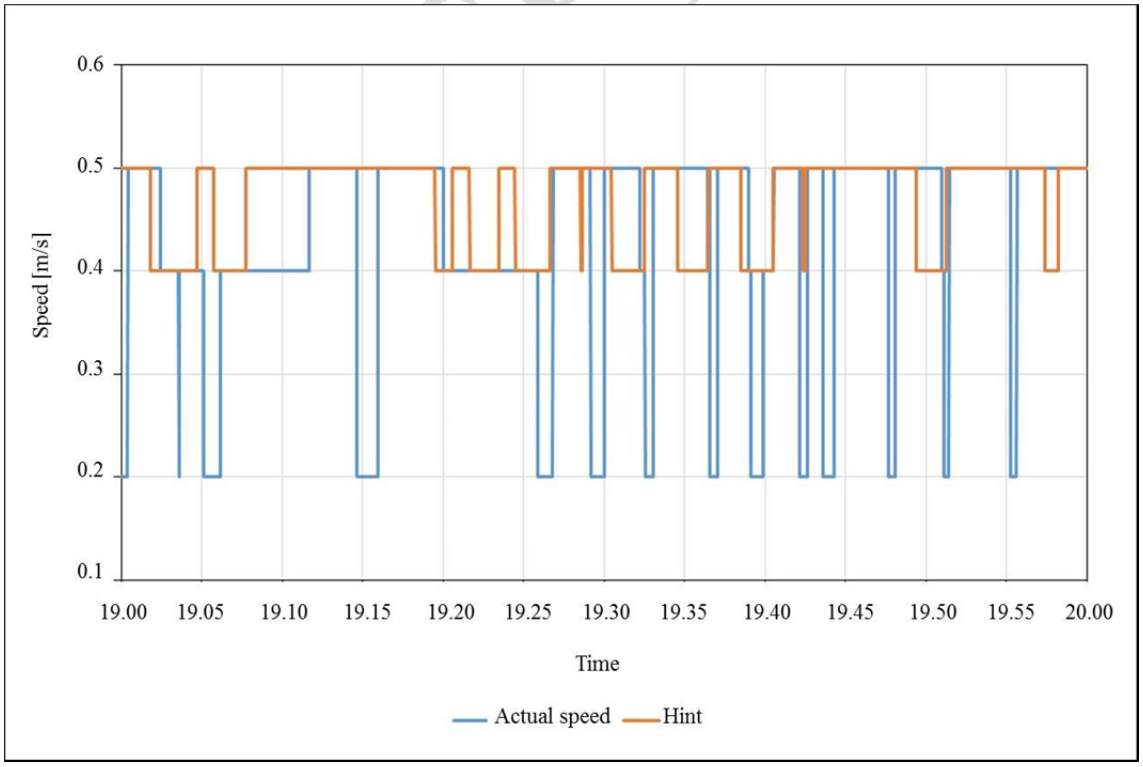


Figure 12. Monitored dynamic trends of speed hint and actual escalator's speed for a time period of one hour.

To sum up, the system acts on 72.54% of the energy consumed by underground stations in public spaces, including the lighting, ventilation and escalator subsystems. The highest energy savings potential was found to be in the forced ventilation, followed by the lighting, and finally by the escalators. Due to the large amount of energy consumed by underground stations, relative percentages are translated into large energy savings in absolute terms (Table 11).

| | **Energy consumption [kWh/year]** | **Potential savings [%]** | **Energy savings [kWh/year]** | |
|---|---|---|---|---|
| | | | **Minimum** | **Maximum** |
| **Private spaces** | **145,768.79** | - | - | - |
| **Public spaces** | **465,629.17** | **17.4±1.4** | **74,336.14** | **87,339.61** |
| Ventilation | 84,193.19 | 30.6±2.0 | 24,079.25 | 27,446.98 |
| Lighting | 214,878.99 | 24.1±1.9 | 47,703.14 | 55,868.54 |
| Escalators | 38,693.20 | 8.5±1.9 | 2,553.75 | 4,024.09 |
| Other | 127,862.92 | - | - | - |
| **Total** | **611,397.96** | **13.2±1.1** | **74,336.14** | **87,339.61** |

Table 11. Energy consumption and potential savings in the prototype underground station.



## 4. CONCLUSIONS

The main outcome of this research is the development and implementation of an intelligent energy management system that can substantially reduce the energy consumption required to operate the main subsystems of underground public spaces. Optimal control is achieved by exploiting synergies with the weather outside, interacting with end users, and predicting near-future states from past experience. Proactive and adaptive control policies for the lighting, ventilation and escalator subsystems are implemented by means of pervasive sensor networks that can create rich representations of the environment. Energy metering and sensor-actuator networks interoperate with existing subsystems in the underground station by means of middleware as an abstraction layer.

The system has been deployed and evaluated in one of the largest underground stations of the Barcelona metro system, giving valuable insight into its applicability in a real scenario. The results obtained during the pilot implementation suggest potential yearly energy savings ranging between 25.86% and 22.01% of the controlled energy, in other words, between 15.96% and 18.76% of the total amount of energy consumed by the public spaces in the underground station. The ventilation subsystem was found to have the highest energy savings potential (30.6 % ± 2.0%), followed by the lighting system (24.1% ± 1.9%) and escalators (8.5% ± 1.9%). In light of the results, it can be concluded that intelligent energy management systems are a competitive alternative for turning metro stations into more sustainable spaces, especially when taking into account

the constraints posed by their underground and urban character and even including the life cycle perspective [37, 38]. Taking into account that this solution can be easily scaled up to the entire network, future research is needed to develop a decision support system to drive mid-term investments within the metro network.

## ACKNOWLEDGEMENTS

This paper is based on results obtained during the SEAM4US project (Sustainable Energy Management for Underground Stations), contract no. 285408 [39]. The research project was supported by the EU FP7 programme (FP7-2011-NMP-ENV-ENERGY-ICT-EeB) and was carried out jointly by the Universita Politecnica delle Marche (Italy), the Universitat Politecnica de Catalunya (Spain), the Fraunhofer Institute for Applied Information Technology (Germany), the VTT Technical Research Centre of Finland (Finland), the University of Kassel (Germany), the TMB - Ferrocarril Metropolita de Barcelona SA (Spain), Cofely Italia SpA (Italy), Almende B.V. (The Netherlands) and CNet Svenska AB (Sweden).

## REFERENCES

[1] Shaikh PH, Nor NBM, Nallagownden P, Elamvazuthi I, Ibrahim T. A review on optimized control systems for building energy and comfort management of smart sustainable buildings. Renew Sust Energ Rev 2014;34:409-429.

[2] Beaudin M, Zareipour H. Home energy management systems: A review of modelling and complexity. Renew Sust Energ Rev 2015;45:318-335.

[3] Khan AA, Razzaq S, Khan A, Khursheed F. HEMSs and enabled demand response in electricity market: An overview. Renew Sust Energ Rev 2015; 42:773-785.

[4] Petri I, Li H, Rezgui Y, Chunfeng Y, Yuce B, Jayan B. A modular optimisation model for reducing energy consumption in large scale building facilities. Renew Sust Energ Rev 2014;38:990-1002.

[5] Papantoniou S, Kolokotsa D, Kalaitzakis K. Building optimization and control algorithms implemented in existing BEMS using a web based energy management and control system. Energ Buildings 2015;98:45-55.

[6] Aghemo C, Virgone J, Fracastoro GV, Pellegrino A, Blaso L, Savoyat J, Johannes K. Management and monitoring of public buildings through ICT based systems: Control rules for energy saving with lighting and HVAC services. Frontiers of Architectural Research 2013;2:147-161.

[7] Gulbinas R, Jain RK, Taylor JE. BizWatts: A modular socio-technical energy management system for empowering commercial building occupants to conserve energy. Appl Energy 2014;136:1076-1084.

[8] Garnier A, Eynard J, Caussanel M, Grieu S.Low computational cost technique for predictive management of thermal comfort in non-residential buildings. J Process Contr 2014, 24:750-762.

[9] European Council (2014). European Council conclusions 23/24 October 2014. Available at: <http://www.consilium.europa.eu/uedocs/cms_data/docs/pressdata/en/ec/145397.pdf>. Accessed on 17 March 2015.

[10] Leung PCM, Lee EWM. Estimation of electrical power consumption in subway station design by intelligent approach. Appl Energy 2013;101:634-643.

[11] González-Gil A, Palacin R, Batty P. Optimal energy management of urban rail systems: Key performance indicators. Energ Convers Manage 2015;90:282–291.
[12] Fuertes A, Casals M, Gangolells M, Puigdollers O. Overcoming challenges for energy management in underground railway stations. The SEAM4US Project. In: eWork and eBusiness in architecture, engineering and construction: proceedings of the 9th European Conference on Product and Process Modelling 2012. Reykjavik, Iceland; July 25-27, 2012.
[13] Casals M, Gangolells M, Forcada N, Macarulla M, Ansuini R. Energy savings in underground metro stations through the implementation of an Environmental Aware Control System. In: eWork and eBusiness in architecture, engineering and construction: proceedings of the 10th European Conference on Product and Process Modelling 2014. Vienna, Austria; September 17-19, 2014.
[14] Casals M, Gangolells M, Forcada N, Macarulla M, Giretti A. A breakdown of energy consumption in underground stations. Energ Buildings 2014;78:89-97.
[15] Lee S, Kim M J, Kim J T, Yoo C K. In search for modeling predictive control of indoor air quality and ventilation energy demand in subway station. Energ Buildings 2015; 98:56-65.
[16] Giretti A, Ansuini R, Casals M, Gangolells M, Amorós F, Valerio C, Pescatori G. Decision support for planning sustainable energy management in underground stations. In: World Sustainable Building Conference 2014. Barcelona, Spain; October 28-30, 2014.
[17] Spain (2007). Royal Decree 1544/2007 regulating the basic conditions of accessibility and no discrimination for accessing and using transport means for disabled people.
[18] Spain (2012). UNE/EN 12464-1:2012 Light and lighting. Work places lighting. Part 1: Indoor work places.
[19] United States Department of Transportation. Subway Environmental Design Handbook: Principles and Applications. 2nd ed. Springfield: National Technical Information Service, 1976.
[20] Ansuini R, Larghetti R, Vaccarini M, Carbonari A, Giretti A, Ruffini S, Guo H, Lau SL. Hybrid modelling for energy saving in subway stations. In: Proceedings of the 2012 Building Simulation and Optimization Conference. Loughborough, United Kingdom; September 10-11, 2012. Available at: < http://www.ibpsa-england.org/resources/files/bso-2012/6C2.pdf >. Accessed on 19 March 2015.
[21] Carbonari A, Vaccarini M, Giretti A. Bayesian networks for supporting model based predictive control of smart buildings. In: Nezhad MSF, editor. Dynamic Programming and Bayesian Inference, Concepts and Applications, InTech; 2014, p. 3-38. Available at: <http://www.intechopen.com/books/dynamic-programming-and-bayesian-inference-concepts-and-applications/bayesian-networks-for-supporting-model-based-predictive-control-of-smart-buildings>. Accessed on 19 March 2015.
[22] Di Perna C, Carbonari A, Ansuini R, Casals M. Empirical approach for real-time estimation of air flow rates in a subway station. Tunn Undergr Space Technol 2014;42:25–39.
[23] Dymola software. Dessault System. Available at: <http://www.3ds.com/products-services/catia/products/dymola/>. Accessed on 2 December 2015
[24] Modelica language. Modelica Association. Available at: <https://www.modelica.org/>. Accessed on 2 December 2015.

[25] Raftery P, Keane M, Costa A. 2011. Calibrating whole building energy models: Detailed case study using hourly measured data. Energ Buildings 2011;43:3666-3679.
[26] Giretti A, Ansuini R, Vaccarini M, Ruffini S. Evidence-based calibration of a subway station model for energy saving. In: Proceedings of the 2014 Building Simulation and Optimization Conference. London, United Kingdom; June 23-24, 2014. Available at: < http://www.bso14.org/BSO14_Papers/BSO14_Paper_036.pdf>. Accessed on 3 December 2015.
[27] ASHRAE (2002). ASHRAE 14-2002: Measurement of energy and demand savings.
[28] Ansuini R, Vaccarini M, Giretti A, Ruffini S. Models for the real-time control of subway stations. In: Proceedings of the 13th Conference of International Building Performance Simulation Association. Chambéry, France; August 25-28, 2013. Available at: < http://www.ibpsa.org/proceedings/BS2013/p_1219.pdf >. Accessed on 9 December 2015.
[29] Sigg S. (2008). Development of a novel context prediction algorithm and analysis of context prediction schemes. University of Kassel (PhD thesis). Available at: <http://www.uni-kassel.de/upress/online/frei/978-3-89958-392-2.volltext.frei.pdf>. Accessed on 3 February 2015.
[30] VTT (2012). AMPASE – A management platform for advanced wireless sensoring. Available at: <http://www.cnl.fi/WSN_tiedostot/Ampase_datasheet_111212.pdf>. Accessed on 3 February 2015.
[31] Efficiency Valuation Organisation (2012). International performance measurement and verification protocol. Concepts and options for determining energy and water savings, vol. 1, Technical Report. Available at: <http://www.nrel.gov/docs/fy02osti/31505.pdf>. Accessed on 3 February 2015.
[32] ASHRAE (2011). International Weather for Energy Calculations (IWEC) files, WMO#081810 - Europe - Original Source Data (c) 2001.
[33] Joint Committee for Guides in Metrology (2008). JCGM 100:2008. Evaluation of measurement data – Guide to the expression of uncertainty in measurement (GUM 1995 with minor corrections).
[34] E4. Energy-Efficient Elevators and Escalators. EU funded project. Contract number: EISAV/EIE/07/111/2007, 2007.
[35] De Almeida A, Hirzel S, Patrão C, Fong J, Dütschke E. Energy-efficient elevators and escalators in Europe: An analysis of energy efficiency potentials and policy measures. Energ Buildings 2012;47:151-158.
[36] Hitachi (2015). Escalators (VX Series). Available at: <http://www.hitachi.com/environment/showcase/solution/industrial/escalator.html >. Accessed on 3 February 2015.
[37] Gangolells M, Casals M, Forcada N, Macarulla M, Giretti A. Environmental impacts related to the commissioning and usage phase of an intelligent energy management system. Appl Energy 2015;138(15):216-223.
[38] Gangolells M, Casals M, Forcada N, Macarulla M, Giretti A. Energy performance assessment of an intelligent energy management system. Renew Sust Energ Rev 2016;55:662-667.
[39] SEAM4US. Sustainable Energy Management for Underground Stations. EU funded project. Contract number: 285408, 2011.